



Published in final edited form as:

Circ Res. 2020 August 28; 127(6): 747–760. doi:10.1161/CIRCRESAHA.120.317086.

Large Extracellular Vesicle-Associated Rap1 Accumulates in Atherosclerotic Plaques, Correlates With Vascular Risks and Is Involved in Atherosclerosis

Liliana Perdomo,

SOPAM, U1063, INSERM, UNIV Angers, SFR ICAT, France

Xavier Vidal-Gómez,

SOPAM, U1063, INSERM, UNIV Angers, SFR ICAT, France

Raffaella Soleti,

SOPAM, U1063, INSERM, UNIV Angers, SFR ICAT, France

Luisa Vergori,

SOPAM, U1063, INSERM, UNIV Angers, SFR ICAT, France

Lucie Duluc,

SOPAM, U1063, INSERM, UNIV Angers, SFR ICAT, France

Maggy Chwastyniak,

Université de Lille, Inserm, CHU Lille, Institute Pasteur De Lille, U1167 - RID-AGE, Lille, France

Malik Bissierier,

Inserm, UMR-1048, Institut Des Maladies Métaboliques et Cardiovasculaires, Toulouse, France

Soazig Le Lay,

SOPAM, U1063, INSERM, UNIV Angers, SFR ICAT, France

Alexandre Villard,

SOPAM, U1063, INSERM, UNIV Angers, SFR ICAT, France

Gilles Simard,

SOPAM, U1063, INSERM, UNIV Angers, SFR ICAT, France

Olivier Meilhac,

DÉTROIT, INSERM U1188, Université de La Réunion, France

Frank Lezoualc'h,

Inserm, UMR-1048, Institut Des Maladies Métaboliques et Cardiovasculaires, Toulouse, France

Ilya Khantalin,

CHU de La Réunion, St Denis, France

Correspondence to: M. Carmen Martínez, PhD, INSERM U1063, Institut de Biologie en Santé, 4 rue Larrey, 49933 Angers, France, carmen.martinez@univangers.fr.

*R.A. and M.C.M. are joint last authors.

Disclosures

None.

The Data Supplement is available with this article at <https://www.ahajournals.org/doi/suppl/10.1161/CIRCRESAHA.120.317086>.

Reuben Veerapen,

Clinique Sainte-Clotilde, Groupe Clinifutur, Sainte-Clotilde, France

Séverine Dubois,

SOPAM, U1063, INSERM, UNIV Angers, SFR ICAT, France

CHU d'Angers, France

Jérôme Boursier,

CHU d'Angers, France

Samir Henni,

CHU d'Angers, France

Frédéric Gagnadoux,

SOPAM, U1063, INSERM, UNIV Angers, SFR ICAT, France

CHU d'Angers, France

Florence Pinet,

Université de Lille, Inserm, CHU Lille, Institute Pasteur De Lille, U1167 - RID-AGE, Lille, France

Ramaroson Andriantsitohaina*,

SOPAM, U1063, INSERM, UNIV Angers, SFR ICAT, France

CHU d'Angers, France

M. Carmen Martínez*

SOPAM, U1063, INSERM, UNIV Angers, SFR ICAT, France

CHU d'Angers, France

Metabol study Group**Abstract**

RATIONALE: Metabolic syndrome (MetS) is a cluster of interrelated risk factors for cardiovascular diseases and atherosclerosis. Circulating levels of large extracellular vesicles (IEVs), submicrometer-sized vesicles released from plasma membrane, from MetS patients were shown to induce endothelial dysfunction, but their role in early stage of atherosclerosis and on vascular smooth muscle cells (SMC) remain to be fully elucidated.

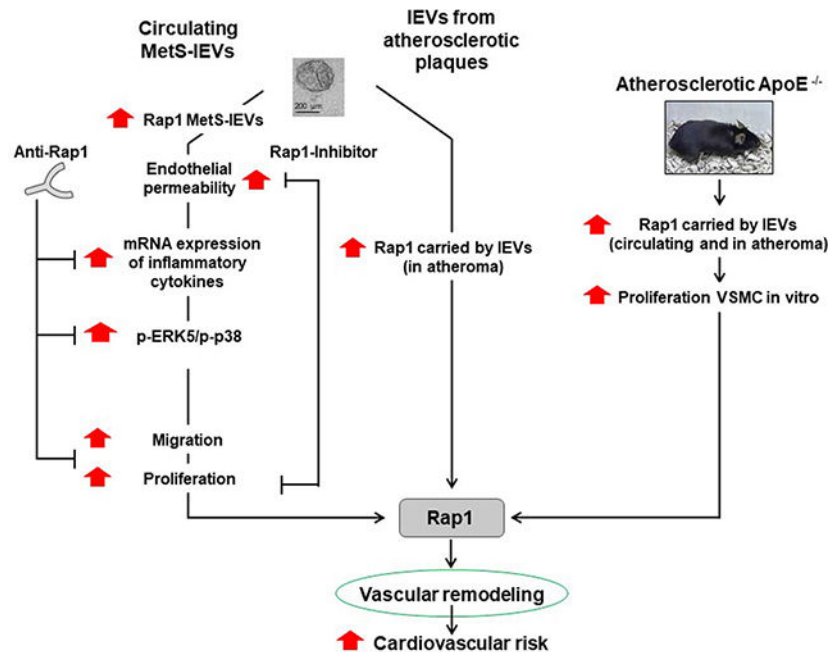
OBJECTIVE: To determine the mechanisms by which IEVs lead to the progression of atherosclerosis in the setting of MetS.

METHODS AND RESULTS: Proteomic analysis revealed that the small GTPase, Rap1 was overexpressed in IEVs from MetS patients compared with those from non-MetS subjects. Rap1 was in GTP-associated active state in both types of IEVs, and Rap1-IEVs levels correlated with increased cardiovascular risks, including stenosis. MetS-IEVs, but not non-MetS-IEVs, increased Rap1-dependent endothelial cell permeability. MetS-IEVs significantly promoted migration and proliferation of human aortic SMC and increased expression of proinflammatory molecules and activation of ERK (extracellular signal-regulated kinase) 5/p38 pathways. Neutralization of Rap1 by specific antibody or pharmacological inhibition of Rap1 completely prevented the effects of

IEVs from MetS patients. High-fat diet-fed ApoE^{-/-} mice displayed an increased expression of Rap1 both in aortas and circulating IEVs. IEVs accumulated in plaque atherosclerotic lesions depending on the progression of atherosclerosis. IEVs from high-fat diet-fed ApoE^{-/-} mice, but not those from mice fed with a standard diet, enhanced SMC proliferation. Human atherosclerotic lesions were enriched in IEVs expressing Rap1.

CONCLUSIONS: These data demonstrate that Rap1 carried by MetS-IEVs participates in the enhanced SMC proliferation, migration, proinflammatory profile, and activation of ERK5/p38 pathways leading to vascular inflammation and remodeling, and atherosclerosis. These results highlight that Rap1 carried by MetS-IEVs may be a novel determinant of diagnostic value for cardiometabolic risk factors and suggest Rap1 as a promising therapeutic target against the development of atherosclerosis.

GRAPHICAL ABSTRACT:



Keywords

atherosclerosis; extracellular vesicles; inflammation; metabolic syndrome; muscle cells

Metabolic syndrome (MetS) patients display an ≈ 2 -fold increased risk of developing atherosclerotic cardiovascular diseases. This syndrome is described as a cluster of abdominal obesity, insulin resistance, elevated blood pressure, and obesity-related dyslipidemia consisting in low levels of HDL-cholesterol and high levels of triglycerides.^{1,2} In the early stages of atherosclerosis, typical human atherosclerotic lesions contain different cell types, including vascular smooth muscle cells (SMC), endothelial cells, fibroblasts, macrophages, and foam cells involved in inflammatory responses and development of plaque.³ Proliferation and migration of vascular SMC from the tunica media to the subendothelial

region, also known as neointima formation play a crucial role in vascular remodeling, a key step for blood vessel thickening and occlusion.⁴

Over the last years, extracellular vesicles (EVs) have been associated with early processes involved in the development of atherosclerotic lesions, including endothelial dysfunction, inflammation, reactive oxygen species production, and monocyte/macrophage adhesion (for review see).⁵ Two main EV subtypes have been described: large EVs (IEVs) released from plasma blebbing and small EVs generated within endosomes forming multivesicular endosomal compartments. Foam cell-derived EVs from atherosclerotic patients were shown to promote SMC migration and adhesion by regulating actin cytoskeleton and focal adhesion pathways after the endocytosis of EVs into SMCs and the subsequent downstream activation of ERK (extracellular signal-regulated kinase) and Akt.⁶ Regarding MetS, we have reported that circulating IEVs from MetS patients (MetS-IEVs) carrying Fas ligand induce endothelial dysfunction by interacting with Fas receptor on endothelial cells; resulting in a temporal crosstalk between endoplasmic reticulum and mitochondria that increased reactive oxygen species production from cytoplasm and mitochondria via the activation of neutral sphingomyelinase and reduced nitric oxide (NO) release.^{7,8} In addition, circulating MetS-IEVs induced hyporeactivity associated with oxidative stress and overexpression of proinflammatory molecules, such as MCP-1 (monocyte chemoattractant protein 1) and inducible NO synthase.⁹ However, the effects of circulating MetS-IEVs, on SMC specifically, in the early stage of atherosclerosis, have not been fully elucidated.

In the present study, proteomic analysis showed that Rap1 was >1.4-fold increased in MetS-IEVs and that IEVs carrying Rap1 induce aortic SMC migration and proliferation as well as proinflammatory cytokine secretion in vitro. All of these effects were abolished when Rap1 carried by IEVs was neutralized or pharmacologically inhibited. Levels of IEVs carrying Rap1 were correlated with waist and hip circumferences, body mass index (BMI), triglyceridemia, insulinemia, hs-CRP (high-sensitivity C-reactive protein), and increased stenosis risk of MetS patients. These results suggested that Rap1 carried by IEVs was critical for the development of atherosclerosis associated with MetS. This was further reinforced by the observation that high-fat diet (HFD)-fed ApoE^{-/-} mice displayed an increased expression of Rap1 in circulating IEVs that also enhanced SMC proliferation. Also, IEVs from mouse and human atherosclerotic plaques were enriched in Rap1. In conclusion, we propose Rap1⁺-IEVs produced in excess as a cause for vascular remodeling and inflammation leading to the progression of atherosclerosis in the setting of MetS.

METHODS

Detailed methods are available in the Data Supplement. The data, analytic methods, and study materials for the purposes of reproducing the results or replicating procedures can be made available on request to the corresponding author who manages the information.

MetS Patients

This study was approved by the ethics committee of the University Hospital of Angers (France). Non-MetS donors (nMetS) and MetS patients were recruited in the NUMEVOX cohort (URL: <https://www.clinicaltrials.gov>. Unique identifier: NCT 00997165). A total of

90 subjects were identified as MetS patients and 72 subjects who displayed 2 or less MetS criteria were identified as nMetS subjects. Baseline characteristics and clinical data of nMetS and MetS subjects are summarized in Table I in the Data Supplement.

Ultrasonography of Carotid Arteries

Velocities and resistance indexes of carotid arteries were determined by duplex ultrasonography following the most recent recommendations of the European Society of Cardiology.

IEV Isolation From Blood

Peripheral blood (20 mL) from nMetS and MetS patients was collected to isolate circulating IEVs and used at the circulating concentration detected for each individual.^{7,8}

Proteomic Study by 2D-DIGE Electrophoresis

Two gels of each were run with a total of 10 µg of mixed fluorescent-labeled proteins per gel containing 5 µg of proteins from IEVs (5 nMetS and 5 MetS patients) randomly labeled with 400 pmol saturation CyDye DIGE (difference gel electrophoresis) fluors (Cy3 or Cy5). After dye-swap, Cy3- and Cy5-labeled samples were mixed and used to rehydrate the immobilized pH gradient strip before perform the isoelectric focusing. After isoelectric focusing, the immobilized pH gradient strips were incubated in equilibration buffer and transferred for the second dimension electrophoresis (SDS-PAGE) onto 12% PAGE gels and sealed with low-melting agarose. Following electrophoresis, gels were scanned with an Ettan DIGE Imager (GE Healthcare) at excitation/emission wavelengths of 532/580 nm for Cy3 and 633/670 nm for Cy5 to yield images with a pixel size of 100 µm. Differentially regulated spots were excised manually from a preparative gel performed with 500 µg of total proteins. Identifications were performed by MALDI-TOF.

Rap Activation Assay

Rap1 pull-down experiments were performed using a GST fusion protein containing the Rap1 binding domain of Ral-GDS.

Characterization of IEV Phenotype

The counting and phenotyping of the MetS-IEVs were performed by flow cytometry from platelet-free plasma according to the expression of membrane-specific antigens.^{7,8} Validation of isolated IEVs was performed by detection of positive and negative markers (Figure IA in the Data Supplement).

Cellular Models

Primary human aortic endothelial cells (Promocell, Heidelberg, Germany) were grown in endothelial basal medium supplemented with 10% of fetal bovine serum. Primary human aortic smooth muscle cells (HASMC, Gibco) were cultured in Medium 231 (Gibco) supplemented with SMGS (Gibco). Primary vascular SMC was obtained from thoracic aorta arteries from WT C57BL/6 male mice, according to number S380 ethic local protocol.

Transepithelial Electric Resistance Measurement of Human Aortic Endothelial Cells

Human aortic endothelial cells were seeded in 8 µm pore size Transwells (Corning, Corning, NY) in the upper chamber until 100% confluence. Transepithelial electric resistance measurement was performed before preincubation with the Rap1 inhibitor and after 24 hours, using a Millicell ERS-2 Voltohmmeter (Merck, Darmstadt, Germany) to assess the integrity of the barrier.

Migration and Proliferation Assays

For wound healing assay, HASMC were cultured in 231-SMGS medium until they achieve 100% confluence. Confluent monolayer was scratched with a sterile pipette tip. Wound healing closure was followed by phase-contrast microscopy at 0 and 24 hours. Also, migration was analyzed by Transwell assay. Cell Proliferation Assay Kit CyQUANT (Invitrogen, Carlsbad, CA) and Ki67 staining were used to analyze proliferation.

Western Blotting

After treatment, HASMCs were homogenized. Equal amounts of proteins were separated in 4% to 15% TGX-midi gels by electrophoresis and then transferred to nitrocellulose sheets. Densitometric analyses of Western blots were performed using ImageJ software.

Quantitative Real-Time Polymerase Chain Reaction Analysis

After treatments, frozen cell pellets were used to analyze the genetic expression of human MCP-1 and IL (interleukin)-6 mRNA by real-time polymerase chain reaction.

Animal Model

All animal studies were performed using approved institutional protocols (no. APAFIS320). Male ApoE^{-/-} were allowed free access to standard diet (STD) or HFD. IEVs were isolated from blood and from atherosclerotic plaque. The effects of circulating IEVs isolated from the ApoE^{-/-} mice on the proliferation of primary SMC isolated from WT mice was evaluated.

Staining and Imaging of Mouse Aorta Wall by Confocal Microscopy

Frozen mouse aortic ring sections were prepared and treated with primary antibodies. Following 3 washes with PBS, secondary antibodies were applied to detect F4/80 and Rap1. Nuclei were counterstained with DAPI. Confocal microscopy and digital image recording were used.

IEVs From Human Atherosclerotic Plaque

Human atherosclerotic plaques from 5 patients undergoing carotid endarterectomy who gave their informed consent were used for IEV isolation.

Statistical Analysis

Data normality was assessed using the Shapiro-Wilk test. Comparisons were made between all conditions for each panel. Statistical analysis was performed by using ANOVA followed by Tukey post hoc test for multiple comparisons. In cases where normality was not

confirmed, statistical analysis from 2 groups and >2 groups were analyzed by the Mann-Whitney *U* test, and Kruskal-Wallis test with Dunn test post hoc, respectively. No experiment-wide multiple test correction was applied. Correlations were performed by Spearman correlation test. Values shown in the text and figures represent the mean \pm the SD or the median (interquartile range) for the clinical data. *P* values were shown in figures and tables. When *P*>0.05, values of *P* were not shown. Statistical analysis was performed using GraphPad Prism (version 5.0; GraphPad Software Inc, San Diego, CA).

RESULTS

MetS patients showed a significant increase in BMI, waist circumference indicating greater visceral obesity, blood pressure, insulinemia, glycemia, glycated hemoglobin, triglycerides, and hs-CRP levels, and decreased plasma HDL levels (Table I in the Data Supplement). In addition, the total number of circulating IEVs was significantly increased in patients with MetS compared with nMetS subjects (Table I in the Data Supplement). As we have previously shown,⁷⁻⁹ MetS patients displayed an increase of \approx 1.7-fold platelet (CD41⁺)-derived IEVs (Table I in the Data Supplement).

Rap1 Activation is Increased in IEVs from Patients with MetS

To identify proteins carried by MetS-IEVs that could play a role in vascular remodeling, we performed a differential proteomic analysis by 2D-DIGE comparing the replicates (Cy3 and Cy5 labeling) prepared from nMetS and MetS. Among the 608 spots detected (Figure IB in the Data Supplement), we found 10 spots differentially expressed (*P*<0.05) between nMetS- and MetS-IEVs (Figure 1A). Identification of proteins present in each spot by MALDI-TOF (Matrix Assisted Laser Desorption Ionization-Time of Flight) allowed us to identify 8 proteins differentially expressed in MetS subjects compared to IEVs isolated from nMetS subjects (Table II in the Data Supplement). Interestingly, spot 534 corresponds to the Ras-related protein Rap1, which has emerged as a central player in cardiovascular pathophysiology.¹⁰ Detailed 2D-spots corresponding to Rap1 is presented for each sample of IEVs from nMetS and MetS patients analyzed (Figure IC in the Data Supplement). We confirmed by immunoblot that MetS-IEVs displayed 50% increase of Rap1 expression compared with nMetS-IEVs (Figure 1B). We also analyzed Rap1 activation by pull-down assay using the Ral-GDS fusion protein in IEVs. Interestingly, we found that MetS-IEVs had higher levels of activated Rap1 (Figure 1C). To determine the location of this protein within the IEVs, Rap1 was analyzed on native or permeabilized MetS-IEVs. As shown in Figure 1D, Rap1 labeling was similar in nonpermeabilized and permeabilized IEVs suggesting that Rap1 is essentially exposed to the surface of IEVs. Thus, further experiments were performed in nonpermeabilized IEVs. Under these conditions, the concentration of circulating IEVs bearing Rap1 was significantly higher in MetS compared with nMetS subjects (Figure 1E). The majority of Rap1⁺-IEVs were also CD41⁺ suggesting that they originated from platelets (Figure 1F). We have also detected low levels of Rap1⁺-EVs from endothelial cells (CD146⁺), erythrocytes (CD235a⁺), leukocytes (CD45⁺), and granulocytes (CD11b⁺). It should be noted that all of these subpopulations of Rap1⁺-IEVs were increased in MetS patients versus nMetS patients. Altogether, these results show that IEVs from MetS patients had higher levels of activated Rap1 at their surface.

Expression Level of Rap1 in IEVs is Closely Correlated with a Cluster of Cardiometabolic Risk Factors in MetS Patients

We analyzed the relationship between circulating levels of IEVs and a cluster of anthropometric parameters and cardiometabolic risk factors (Figure 2). Neither total circulating IEVs nor platelet- and endothelial-derived IEVs were correlated with any of these parameters (not shown). Interestingly, circulating IEVs carrying Rap1 were positively correlated with waist and hip circumferences, BMI ($r=0.1936$, $P=0.0219$), the mean heart rate, insulinemia, plasma triglyceride concentration, and hs-CRP concentration (Figure 2A through 2F). Consistently, the TyG (triglyceride-glucose) index was also positively correlated with the circulating level of Rap1-IEVs in MetS (Figure 2G), reflecting insulin resistance in these patients.

Vascular parameters, such as aorta diameter or pulse wave velocity, did not correlate with the number of MetS criteria neither with IEVs carrying Rap1 (not shown). Interestingly, the right common carotid end-diastolic velocity was positively correlated with the levels of Rap1-IEVs (Figure 2H). Finally, the analysis performed on 162 subjects displaying 0 to 5 of MetS criteria showed that circulating levels of IEVs carrying Rap1 increased depending on the number of the components of MetS, thus its severity (Figure 2I). These data suggest that circulating levels of Rap1 carried by MetS-IEVs are associated with risk factors of cardiovascular events in MetS patients, identifying Rap1 carried by MetS-IEVs as a potential molecular link leading to the development of vascular diseases, such as atherosclerosis.

IEVs from MetS Patients Increase Endothelial Cell Permeability Sensitive to the Rap1 Inhibitor

Incubation for 24 hours with IEVs from MetS patients decreased transendothelial electrical resistance, whereas those from nMetS patients had not significant effects (Figure 3A). Interestingly, the pharmacological Rap1 inhibition with the geranylgeranyltransferase I inhibitor-298 (GGTi-298), improved MetS-IEVs-induced reduction of transepithelial electric resistance values (Figure 3A). In addition, MetS-IEVs increased monocyte transcytosis through the endothelial cell monolayer, and this effect was prevented by GGTi-298 (Figure 3B). Altogether, these data indicate that IEVs from MetS patients, but not those from nMetS patients, enhance endothelial permeability by a mechanism sensitive to GGTi-298. These results also suggest that MetS-IEVs can reach SMC into the vessel through this pathway.

Rap1 Carried by Circulating IEVs Induces Migration and Proliferation of HASMCs

To decipher the interaction between IEVs and vascular SMC, we studied IEV internalization in HASMC by confocal microscopy and showed that IEVs from nMetS and MetS patients labeled with PKH67 were internalized by HASMC after 4 hours of incubation (Figure IIA in the Data Supplement). To study the role of Rap1 carried by IEVs on HASMC and vascular remodeling, we measured HASMC migration induced by nMetS- and MetS-IEVs by wound healing assay. MetS-IEVs, but not nMetS-IEVs, significantly increased HASMC migration (Figure 3C and 3D). Preincubation of MetS-IEVs with Rap1 antibody abolished HASMC migration induced by MetS-IEVs (Figure 3C and 3D). Similar results were obtained by Transwell assays (Figure IIB and IIC in the Data Supplement). Positive controls using PDGF (platelet-derived growth factor) or 8-(4-Chlorophenylthio) adenosine 3',5'-cyclic

monophosphate sodium salt (8-CPT), (an activator of Rap1-GTP via the exchange factor Epac), are shown in Figure III in the Data Supplement both for migration and proliferation.

MetS-IEVs, but not nMetS-IEVs, significantly increased the number of HASMCs, and this effect was abolished by neutralization of Rap1 (Figure 3E). In line with these findings, the increase of cell number induced by MetS-IEVs was abolished in the presence of the Rap1 pharmacological inhibitor, GGTi-298 (Figure 3F). Similar results were observed when HASMC proliferation was measured by Ki67 staining assay (Figure IIE in the Data Supplement). Altogether, these results suggest that Rap1 carried by IEVs from MetS plays a critical role in migration and proliferation of HASMC, as general features of vascular remodeling.

Rap1 Carried by IEVs Activates MEK5-ERK5 and p38 Pathways to Induce Proliferation of HASMCs

Since the mechanisms underlying the crosstalk between small GTPase proteins and MAPK (mitogen-activated protein kinase) signaling have also been intensively investigated,¹¹ we analyzed the effects of MetS-IEVs on MAPKs signaling pathway in HASMC, with a particular focus on ERK1/2, ERK5, and p38 MAPK. Neither PDGF, 8-CPT, nMetS-IEVs, nor MetS-IEVs increased phosphorylation of ERK1/2 (Figure IVA and IVB in the Data Supplement). Interestingly, PDGF, 8-CPT, MetS-IEVs, but not nMetS-IEVs, significantly increased ERK5 phosphorylation (Figure 4A and 4B) which was significantly reduced after neutralization of Rap1 (Figure 4A and 4B). Moreover, the ability of MetS-IEVs to enhance the number of HASMC was abrogated in the presence of ERK5 inhibitor, BIX02189 (Figure 4C). These data suggest that the ERK5 pathway triggers the ability of IEVs from MetS carrying Rap1 to increase HASMC proliferation. Finally, MetS-IEVs, but not PDGF, 8-CPT or nMetS-IEVs, increased p38 MAPK phosphorylation in HASMC, and this effect was inhibited after neutralization of Rap1 carried by MetS-IEVs (Figure 4A and 4B). Altogether, these results showed that ERK5 and p38 MAPK, but not ERK1/2, were activated by MetS-IEVs in HASMC.

MetS-IEVs Increase MCP-1 and IL-6 Expression in a Rap1-Dependent Manner

Rap1 is an important regulator of the vascular inflammatory response.¹⁰ To confirm the contribution of Rap1-IEVs on the inflammatory response observed during MetS, the effects of nMetS-IEVs and MetS-IEVs were tested on mRNA expression of different proinflammatory cytokines in HASMC. We found that MetS-IEVs, but not nMetS-IEVs, significantly increased mRNA expression of MCP-1 and IL-6 (Figure 5A and 5B). Neutralizing Rap1 carried by MetS-IEVs completely abrogated their ability to increase MCP-1 and IL-6 mRNA expressions in HASMC (Figure 5A and 5B). In contrast, neither MetS-IEVs nor nMetS-IEVs modified VCAM-1 (vascular cell adhesion molecule-1) and ICAM-1 (intercellulaire adhesion molecule-1) protein expressions and NF- κ B (nuclear factor kappa-light-chain-enhancer of activated B cells) pathway activation (Figure IVC in the Data Supplement). These data suggest that MetS-IEVs increase the expression of inflammatory cytokines, MCP-1, and IL-6, which have been previously described to be overexpressed in patients with increased cardiovascular risk factors.

Pathophysiological Relevance of Rap1 in the Atherosclerotic Process

To study the pathophysiological relevance of Rap1 in the atherosclerotic process, we used the HFD-fed ApoE^{-/-} mouse model, exhibiting an exacerbation of the formation of atherosclerotic lesions. Macrophage infiltration was analyzed by confocal microscopy by staining of F4/80 together with the expression of Rap1 in aortic roots from STD- and HFD-fed ApoE^{-/-} mice. We observed an enhanced macrophage infiltration in aorta of HFD-fed ApoE^{-/-} mice when compared with STD-fed ApoE^{-/-} mice (Figure 6A and 6B). Rap1 staining was increased in the medial layer of the aorta from HFD-fed ApoE^{-/-} compared with that from STD-fed ApoE^{-/-} mice (Figure 6A and 6B). Circulating IEVs from HFD-fed ApoE^{-/-} displayed greater expression of Rap1 compared with those from STD-fed ApoE^{-/-} mice (Figure 6C). Interestingly, circulating IEVs from HFD-fed ApoE^{-/-} mice, but not those from STD-fed ApoE^{-/-}, enhanced the number of primary murine aortic SMC (Figure 6D).

We tested whether IEVs expressing Rap1 were localized in atherosclerotic plaques in ApoE^{-/-} mice. For this, IEVs were isolated from atherosclerotic plaques and characterized by flow cytometry. IEVs essentially were from SMC (74%), leukocytes (11%), macrophages (5%), and platelets (6%; Figure V in the Data Supplement). In addition, atherosclerotic aortic plaques from HFD-fed ApoE^{-/-} mice contained higher levels of IEVs carrying Rap1 than arterial wall of aorta from STD-fed ApoE^{-/-} mice (Figure 6E). Interestingly, the content of Rap1⁺-IEVs increased depending on the stage of plaque development, being similar at 8, 12, or 16 weeks in STD-fed mice but increasing between 12 and 16 weeks in HFD-fed mice (Figure 6E). These results indicate that accumulation of Rap1⁺-IEVs in atheroma plaques is associated with the progression of the atherosclerotic plaque in ApoE^{-/-} mice and strengthened our hypothesis that Rap1 carried by circulating IEVs plays a role in the development of atherosclerosis in HFD-fed ApoE^{-/-} mice.

Finally, we analyzed the presence of Rap1⁺-IEVs on human atherosclerotic plaque samples. Rap1⁺-IEVs were more abundant in human atherosclerotic plaques than in the arterial wall adjacent to the lesion (Figure 7). The analysis of the content of IEVs from human atherosclerotic plaque showed that they were mainly originated from SMC (42%), leukocytes (19%), platelets (16%), and endothelial cells (14%; Figure V in the Data Supplement). These results corroborate that IEVs expressing Rap1 accumulate in atherosclerotic lesions.

DISCUSSION

The present study highlights the role of circulating IEVs carrying Rap1 as a crucial driver of the early steps of atherosclerosis, such as SMC hyperplasia and inflammation in MetS. Circulating MetS-IEVs, but not nMetS-IEVs, increased endothelial cell permeability and monocyte transcytosis suggesting that, in vivo, they can reach smooth muscle layer into the vessels. In addition, we demonstrated that MetS-IEVs overexpressed the small protein GTPase Rap1 on the surface of IEVs in its active GTP-bound form. Moreover, circulating levels of Rap1-IEVs were not only positively correlated with the severity of MetS and obesity indicators, such as waist and hip circumferences and BMI, but also with risk factors to develop cardiovascular diseases, such as Increased heart rate, hyperinsulinemia, hypertriglyceridemia, TyG index, hs-CRP, and right common carotid end-diastolic velocity.

At the cellular and molecular level, IEVs carrying Rap1 induced SMC migration and proliferation by a mechanism involving the Rap1/ERK5 axis and proinflammatory profile. Finally, by using a mouse model of atherosclerosis and plaques from patients undergoing carotid endarterectomy, we showed that IEVs carrying Rap1 accumulated in atherosclerotic lesions strongly supporting the critical role of Rap1 carried by IEVs in vascular remodeling leading to atherosclerosis. Since SMC hyperplasia is a critical mechanism involved in the early steps of atherosclerosis, Rap1 carried by IEVs could represent a promising therapeutic target to limit the development of atherosclerosis through the reduction of both SMC proliferation and SMC proinflammatory profile.

MetS criteria, including central obesity, hypertension, hyperglycemia, hypertriglyceridemia, and low HDL levels, are commonly associated with the risk of developing atherosclerosis and cardiovascular events.¹² However, there is no existing valid biomarker to accurately predict the risk of developing cardiovascular diseases since it is difficult to demonstrate the relationship between cardiovascular diseases and each MetS criterion, as they overlap. EVs are important players in intercellular communication and have been described as potential biomarkers in different pathologies, such as diabetes mellitus and obesity. It has been recently reported that EVs have an impact on cardiovascular physiology and atherothrombotic events.^{12,13} Interestingly, IEVs have been highlighted as important actors during the initiation and the progression of atherosclerotic lesions due to their capacity to interact with endothelial cells, SMC, and circulating cells, such as monocytes.⁵

In the present study, we showed that IEVs isolated from MetS patients had higher levels of activated Rap1 at their surface compared with nMetS-IEVs. It has been shown that when Rap1 is localized in the plasma membrane, the GTPase is activated, whereas the intracellular pool of Rap remained GDP-bound and, in consequence, not activated.^{14,15} Since Rap1 is detected by flow cytometry without permeabilization of IEVs, we hypothesize that activated Rap1 is present at the membrane of IEVs and that probably limits the ability of Rap1 to cycle between the GDP- and GTP-bound states. We also demonstrated that circulating levels of IEVs carrying Rap1 increased depending on the severity of MetS, and positively correlated with abdominal obesity and BMI, and with the cardiovascular risk factors, including enhanced heart rate, hyperinsulinemia, hypertriglyceridemia, and TyG index reflecting insulin resistance. These findings corroborate previous work of our team showing that obese patients displayed enhanced levels of circulating IEVs,¹⁶ and strongly suggest that IEVs expressing Rap1 might be useful to early Identify Individuals at a high risk of developing cardiovascular events. In this context, Cooney et al¹⁷ have shown that the cardiovascular risk associated with each 15 beats/min increase in resting heart rate was 1.24 in men and 1.32 in women, demonstrating a relationship between heart rate and incident cardiovascular. Also, hyperinsulinemia can predict adverse cardiac events in type 2 diabetes mellitus,¹⁸ hypertriglyceridemia is an independent marker of ischemic events risk,¹⁹ while TyG index can identify early individuals at a high risk of developing cardiovascular events.²⁰ Levels of IEVs carrying Rap1 also correlated with levels of hs-CRP which is a described marker to estimate the risk of plaque instability²¹ and vulnerability of atheromatous lesion.²² To corroborate this, IEVs carrying Rap1 were also correlated with right common carotid end-diastolic velocity, which is associated with a high probability to develop stenosis.²³ All

these clinical data strongly support that circulating levels of IEVs harboring Rap1 could be useful to evaluate the risks of developing cardiovascular events in MetS patients.

Our data show that MetS-IEVs, but not those from nMetS patients, enhanced endothelial permeability and monocyte transcytosis by a mechanism sensitive to GGTi-298 suggesting that MetS-IEVs can reach SMC into the vessel. In line with these results, we have previously reported that lymphocyte-derived IEVs injected in vivo were able to interact directly with SMC as evidenced by an increased CD4 labeling in the media layer of aortas from IEV-treated mice compared with control vessels.²⁴ We also found that intravenous injection of MetS-IEVs into mice induced vascular hyporeactivity that is associated with upregulation of inducible NO-synthase and increased production of NO.⁹

Activation of Rap1 was associated with the enhancement of vascular SMC migration in vitro and the development of neointimal thickening in fetal rat aortic tissues in organ culture.²⁵ To confirm the involvement of Rap1 carried by IEVs in the early stages of atherosclerosis, we analyzed the effects of IEVs on HASMC migration, proliferation, and cytokine production. Our findings show that MetS-IEVs significantly increased the migration and the proliferation of HASMC via a mechanism involving Rap1 and the subsequent activation of ERK5. We observed that the effects of Rap1 carried by MetS-IEVs on HASMC proliferation were inhibited by using a selective small-molecule ATP-site inhibitor of MEK5/ERK5 signaling, BIX02189. These results are in accordance with a recent study published by Li et al²⁶ suggesting that transfection with the activated Rap1 protein directly modulates the phosphorylation of ERK pathways and promotes proliferation, differentiation, and migration of vascular SMC. Indeed, as other small G proteins, Rap1 is able to directly activate several MAPKs. In this respect, it has been shown that, in cortical neurons, constitutive active Rap1 is sufficient to activate ERK5 via the MEKK2-MEK5 signaling cascade.²⁷ ERK5 has also been described as a central mediator of TLR (toll-like receptor)-2-dependent inflammatory signaling in human endothelial cells and monocytes; and activation of TLR-2 led to the upregulation of inflammatory mediators via NF- κ B, JNK (c-Jun N-terminal kinase), and p38 MAPK, promoting the attachment of human neutrophils to lung microvascular endothelial cells.²⁸ We also looked at p38 MAPK activation, which has been previously associated with the development and progression of atherosclerosis by upregulating migration, proliferation, permeability, apoptosis, and adhesion molecule expression in endothelial cells.²⁹ It has also been described that an increase of Rap1 mediated by p38 MAPK activation enhanced migration and invasion in fibroblasts.³⁰ Similar to ERK5, we observed that MetS-IEVs increased p38 MAPK phosphorylation, which was prevented upon Rap1 neutralization. Migration and proliferation processes are altered during vascular remodeling as part of the reparative response to injury and can lead to neointimal formation associated with infiltration of inflammatory cells and matrix production.³¹ Furthermore, our findings showed that MetS-IEVs, by a Rap1-dependent mechanism, increased mRNA expression of the proinflammatory cytokines MCP-1 and IL-6, which were described to be involved in the development of atherosclerosis.³² Neither MetS-IEVs nor nMetS-IEVs modified VCAM-1 and ICAM-1 expression and NF- κ B pathway activation. Several hypotheses can be advanced to explain these findings. Thus, it has been described that whereas VCAM-1 and ICAM-1 expression is mainly regulated by NF- κ B pathway,³³ IL-6 and MCP-1 release can be regulated by other transcription factors different to NF- κ B, such as CREB (c-AMP response

element-binding protein)³⁴ or AP-1 (activator protein-1).³⁵ Nevertheless, these results and those previously described⁹ showing an increased MCP-1 expression in the aorta after intravenous injection of MetS-IEVs into mice suggest that MetS-IEVs could potentially increase the recruitment of proinflammatory circulating cells, such as leukocytes, under conditions associated with vascular inflammation.

Finally, by using an animal model prone to the atherosclerotic lesion, the HFD-fed ApoE^{-/-} mouse model, we confirmed the crucial role of Rap1 in the development of atherosclerosis. We showed that the aorta of HFD-fed ApoE^{-/-} mice displayed enhanced expression of Rap1 and macrophage infiltration. In addition, Rap1 was overexpressed in circulating IEVs from atherosclerotic mice; and that these IEVs induced proliferation of murine aortic SMC. Moreover, since the content of Rap1⁺-IEVs increased depending on the stage of plaque development in HFD-fed mice and Rap1-IEVs accumulated in atherosclerotic lesions from humans undergoing carotid endarterectomy, our results strongly suggest the involvement of Rap1-IEVs in the progression of atherosclerosis.

Limitations

A large number of patients declined to participate in the vascular function analysis. Accordingly, vascular function measurements were performed only on 20% of nMetS subjects and 50% of MetS patients. Although the number of patients is low, significant correlation between IEVs carrying Rap1 and right common carotid end-diastolic velocity was found suggesting that this vascular parameter is strongly associated with IEVs expressing Rap1. Also, it should be noted that 73% of nMetS patients displayed 1 or 2 criteria of MetS, and this could explain the trend to increase SMC migration and proliferation induced by IEVs from nMetS patients. Nevertheless, the effects of IEVs from nMetS patients were not significant and never prevented when Rap1 in nMetS-IEVs was neutralized or inhibited suggesting that Rap1 does not account for these effects. In addition, the fact that nMetS-IEVs did not increase endothelial cell permeability strongly suggests that the ability of circulating nMetS-IEVs to reach smooth muscle layer under in vivo conditions is very restricted. The present study shows the crucial role of Rap1 carried by IEVs on the processes involved in SMC remodeling, including SMC proliferation, migration, and secretion of proinflammatory cytokines; however, the molecular link between Rap1 and proinflammatory cytokine production needs to be further explored. Several approaches may be used but none with optimal results. First, although constitutive Rap1^{-/-} mice are available, their use cannot help us since whole-body knockout implicates the lack of Rap1 also in target SMC. Another possibility is the use of Rap1 plasmids to overexpress Rap1; however, in this case, only one type of cells generating Rap1-enriched IEVs will be transfected, and in the present study, IEVs overexpressing Rap1 are from several cell-type origin (Figure 1F). Nonetheless, we demonstrate by using a specific antibody and a pharmacological inhibitor the involvement of Rap1 carried by IEVs from MetS patients in the early steps of atherosclerosis.

In conclusion, circulating IEVs from MetS patients had higher levels of activated Rap1 protein and that correlated with cardiovascular risk factors. MetS-IEVs carrying Rap1 increased mRNA expression of MCP-1 and IL6 as well as the phosphorylation level of

ERK5 and p38 MAPK. By activating ERK-MAPK pathways, MetS-IEVs induced the migration and proliferation of SMC, processes involved in vascular remodeling. All of these effects were reduced or abolished when Rap1 was neutralized or pharmacologically blocked. In vivo, atherosclerotic HFD-fed ApoE^{-/-} also displayed high expression of Rap1 in circulating IEVs which also promoted proliferation of murine aortic SMC. Since we have previously shown that, in endothelial cells, MetS-IEVs induce endoplasmic reticulum stress associated with an increase of oxidative stress through the activation of the Fas/Fas ligand pathway,⁸ the results of the present study highlight the deleterious effects of these IEVs on vascular cells. In this respect, it has been shown that the Fas/Fas ligand pathway triggers activation of Rap1 signaling leading to integrin activation, and then, the induction of proinflammatory cell recruitment.³⁶ Thus, in a more integrative model, MetS-IEVs act first on the endothelial cells and through both Fas/Fas ligand and Rap1 pathway they evoke the decrease in NO production and the increase on endothelial cell permeability; second, MetS-IEVs reach SMC and favor early steps of atherosclerosis. Taken together, these results support the hypothesis that Rap1⁺-IEVs produced in excess could represent a promising therapeutic target to prevent or limit the progression of atherosclerosis in MetS subjects, as well as a biomarker to predict vascular consequences of MetS.

Supplementary Material

Refer to Web version on PubMed Central for supplementary material.

Acknowledgments

We thank S. Marechal-Girault and P. Vandeputte for analysis of clinical data of Numevox cohort and the staff of SCAHU (Angers) for the care of animals. Also, we thank G. Hilaret, P. Mallegol, and C. Besnard for help in confocal microscopy analysis, polymerase chain reaction (PCR) experiments, and flow cytometry measurements, respectively. Metabol Study Group Composition: CLINICS (Centre Hospitalo-Universitaire d'Angers (CHU), Angers, France): Hepatology: Jérôme Boursier, Paul Calès, Frédéric Oberti, Isabelle Fouchard-Hubert, and Adrien Lannes; Diabetology: Séverine Dubois, Ingrid Allix, and Pierre-Henri Ducluzeau; Pneumology: Frédéric Gagnadoux, Wojciech Trzepizur, Nicole Meslier, and Pascaline Priou; Functional Vascular Explorations: Samir Henni, Georges Leftheriotis, and Pierre Abraham; and Radiology: Christophe Aubé. BASIC SCIENCE (INSERM U1063, SOPAM, Angers University, France): Ramarosan Andriantsitohaina, M. Carmen Martinez, Soazig Le Lay, Raffaella Soleti, and Luisa Vergori. STATISTICS: Gilles Hunault. BIOLOGICAL RESSOURCE CENTER: Odile Blanchet and Belaid Sekour. COORDINATION: Jean-Marie Chrétien and Sandra Girre. L. Perdomo, X. Vidal-Gomez, R. Soleti, L. Vergori, L. Duluc, M. Chwastyniak, M. Bisserier, and A. Villard conducted experiments, acquired data, analyzed data; F. Pinet performed proteomic analysis; F. Lezoualc'h performed Rap activation assay; S. Le Lay, G. Simard discussed the study; S. Dubois, J. Boursier, S. Henni, F. Gagnadoux, O. Meilhac, I. Khantaline, and R. Veerapen provided human samples; R. Andriantsitohaina, and M.C. Martinez conceived and supervised the study, designed the experiments; and L. Perdomo, R. Andriantsitohaina, and M.C. Martinez wrote the article.

Sources of Funding

This work was supported by INSERM, Université d'Angers and CHU Angers. L. Perdomo was recipient of a post-doctoral fellowship from Angers Loire Metropole and A. Villard a doctoral fellowship from Région Pays de la Loire. X. Vidal-Gomez was supported by Fondation pour la Recherche Médicale (SPF201809006985).

Nonstandard Abbreviations and Acronyms

8-CPT	8-(4-Chlorophenylthio) adenosine 3',5'-cyclic monophosphate sodium salt
BMI	body mass index

EVs	extracellular vesicles
HASMC	human aortic smooth muscle cells
HFD	high-fat diet
hs-CRP	high-sensitivity C-reactive protein
IL	interleukin
IEVs	large extracellular vesicles
MCP-1	monocyte chemoattractant protein 1
MetS	metabolic syndrome
MetS-IEVs	circulating large extracellular vesicles from MetS patients
nMetS	non-metabolic syndrome
nMetS-IEVs	circulating large extracellular vesicles from nMetS patients
NO	nitric oxide
PDGF	platelet-derived growth factor
SMC	smooth muscle cells
STD	standard diet
TyG index	triglyceride-glucose index

REFERENCES

- Harris MF. The metabolic syndrome. *Aust Fam Physician*. 2013;42:524–527. [PubMed: 23971058]
- Alberti KG, Eckel RH, Grundy SM, Zimmet PZ, Cleeman JI, Donato KA, Fruchart JC, James WP, Loria CM, Smith SC Jr; International Diabetes Federation Task Force on Epidemiology and Prevention; National Heart, Lung, and Blood Institute; American Heart Association; World Heart Federation; International Atherosclerosis Society; International Association for the Study of Obesity. Harmonizing the metabolic syndrome: a joint interim statement of the International Diabetes Federation Task Force on Epidemiology and Prevention; National Heart, Lung, and Blood Institute; American Heart Association; World Heart Federation; International Atherosclerosis Society; and International Association for the Study of Obesity. *Circulation*. 2009;120:1640–1645. doi: 10.1161/CIRCULATIONAHA.109.192644 [PubMed: 19805654]
- Ross R Atherosclerosis-an inflammatory disease. *N Engl J Med*. 1999;340:115–126. doi: 10.1056/NEJM199901143400207 [PubMed: 9887164]
- Bentzon JF, Otsuka F, Virmani R, Falk E. Mechanisms of plaque formation and rupture. *Circ Res*. 2014;114:1852–1866. doi: 10.1161/CIRCRESAHA.114.302721 [PubMed: 24902970]
- Mallici M, Perdomo L, Veerasamy M, Andriantsitohaina R, Simard G, Martínez MC. Extracellular vesicles: mechanisms in human health and disease. *Antioxid Redox Signal* 2019;30:813–856. doi: 10.1089/ars.2017.7265 [PubMed: 29634347]
- Niu C, Wang X, Zhao M, Cai T, Liu P, Li J, Willard B, Zu L, Zhou E, Li Y, et al. Macrophage foam cell-derived extracellular vesicles promote vascular smooth muscle cell migration and adhesion. *J Am Heart*. 2016;5:e004099. doi: 10.1161/JAHA.116.004099
- Agouni A, Lagrue-Lak-Hal AH, Ducluzeau PH, Mostefai HA, Draunet-Busson C, Leftheriotis G, Heymes C, Martinez MC, Andriantsitohaina R. Endothelial dysfunction caused by circulating

- microparticles from patients with metabolic syndrome. *Am J Pathol.* 2008;173:1210–1219. doi: 10.2353/ajpath.2008.080228 [PubMed: 18772329]
8. Safiedeen Z, Rodríguez-Gómez I, Vergori L, Soleti R, Vaithilingam D, Douma I, Agouni A, Leiber D, Dubois S, Simard G, et al. Temporal cross talk between endoplasmic reticulum and mitochondria regulates oxidative stress and mediates microparticle-induced endothelial dysfunction. *Antioxid Redox Signal.* 2017;26:15–27. doi: 10.1089/ars.2016.6771 [PubMed: 27392575]
 9. Agouni A, Ducluzeau PH, Benameur T, Faure S, Sladkova M, Duluc L, Leftheriotis G, Pechanova O, Delibegovic M, Martinez MC, et al. Microparticles from patients with metabolic syndrome induce vascular hypo-reactivity via Fas/Fas-ligand pathway in mice. *PLoS One.* 2011;6:e27809. doi: 10.1371/journal.pone.0027809 [PubMed: 22110764]
 10. Métrich M, Berthouze M, Morel E, Crozatier B, Gomez AM, Lezoualc'h F. Role of the cAMP-binding protein Epac in cardiovascular physiology and pathophysiology. *Pflugers Arch.* 2010;459:535–546. doi: 10.1007/s00424-009-0747-y [PubMed: 19855995]
 11. Romano D, Magalon K, Ciampini A, Talet C, Enjalbert A, Gerard C. Differential involvement of the Ras and Rap1 small GTPases in vasoactive intestinal and pituitary adenylyl cyclase activating polypeptides control of the prolactin gene. *J Biol Chem.* 2003;278:51386–51394. doi: 10.1074/jbc.M308372200 [PubMed: 14551200]
 12. Barrachina MN, Calderón-Cruz B, Fernandez-Rocca L, García Á. Application of extracellular vesicles proteomics to cardiovascular disease: guidelines, data analysis, and future perspectives. *Proteomics.* 2019;19:e1800247 doi: 10.1002/pmic.201800247 [PubMed: 30467982]
 13. Martínez MC, Andriantsitohaina R. Extracellular vesicles in metabolic syndrome. *Circ Res* 2017;120:1674–1686. doi: 10.1161/CIRCRESAHA.117.309419 [PubMed: 28495997]
 14. Bivona TG, Wiener HH, Ahearn IM, Silletti J, Chiu VK, Philips MR. Rap1 upregulation and activation on plasma membrane regulates T cell adhesion. *J Cell Biol.* 2004;164:461–470. doi: 10.1083/jcb.200311093 [PubMed: 14757755]
 15. Torti M, Lapetina EG. Structure and function of rap proteins in human platelets. *Thromb Haemost.* 1994;71:533–543. [PubMed: 8091376]
 16. Amosse J, Durcin M, Mallocci M, Vergori L, Fleury A, Gagnadoux F, Dubois S, Simard G, Boursier J, Hue O, et al. Phenotyping of circulating extracellular vesicles (EVs) in obesity identifies large EVs as functional conveyors of macrophage migration inhibitory factor. *Mol Metab.* 2018;18:134–142. doi: 10.1016/j.molmet.2018.10.001 [PubMed: 30473096]
 17. Cooney MT, Vartiainen E, Laatikainen T, Laakitainen T, Juolevi A, Dudina A, Graham IM. Elevated resting heart rate is an independent risk factor for cardiovascular disease in healthy men and women. *Am Heart J.* 2010;159:612–619.e3. doi: 10.1016/j.ahj.2009.12.029 [PubMed: 20362720]
 18. Srinivasan M, Kamath P Bhat N, Pai N, Bhat R, Shah T, Manjrekar P, Mahabala C. Basal hyperinsulinemia beyond a threshold predicts major adverse cardiac events at 1 year after coronary angiogram in type 2 diabetes mellitus: a retrospective cohort study. *Diabetol Metab Syndr.* 2017;9:38. doi: 10.1186/s13098-017-0237-x [PubMed: 28529547]
 19. Toth PP, Granowitz C, Hull M, Liassou D, Anderson A, Philip S. High triglycerides are associated with increased cardiovascular events, medical costs, and resource use: a real-world administrative claims analysis of statin-treated patients with high residual cardiovascular risk. *J Am Heart Assoc.* 2018;7:e008740. doi: 10.1161/JAHA.118.008740 [PubMed: 30371242]
 20. Sánchez-Iñigo L, Navarro-González D, Fernández-Montero A, Pastrana-Delgado J, Martínez JA. The TyG index may predict the development of cardiovascular events. *Eur J Clin Invest.* 2016;46:189–197. doi: 10.1111/eci.12583 [PubMed: 26683265]
 21. Alvarez Garcia B, Ruiz C, Chacon P Sabin JA, Matas M. High-sensitivity C-reactive protein in high-grade carotid stenosis: risk marker for unstable carotid plaque. *J Vasc Surg.* 2003;38:1018–1024. doi: 10.1016/s0741-5214(03)00709-2 [PubMed: 14603210]
 22. Zhong ZX, Li B, Li CR, Zhang QF, Liu ZD, Zhang PF, Gu XF, Luo H, Li MJ, Luo HS, et al. Role of chemokines in promoting instability of coronary atherosclerotic plaques and the underlying molecular mechanism. *Braz J Med Biol Res.* 2015;48:161–166. doi: 10.1590/1414-431X20144195 [PubMed: 25424368]

23. Strosberg DS, Haurani MJ, Satiani B, Go MR. Common carotid artery end-diastolic velocity and acceleration time can predict degree of internal carotid artery stenosis. *J Vasc Surg*. 2017;66:226–231. doi: 10.1016/j.jvs.2017.01.041 [PubMed: 28390773]
24. Tesse A, Martínez MC, Hugel B, Chalupsky K, Muller CD, Meziani F, Mitolo-Chieppa D, Freyssinet JM, Andriantsitohaina R. Upregulation of proinflammatory proteins through NF-kappaB pathway by shed membrane microparticles results in vascular hyporeactivity. *Arterioscler Thromb Vasc Biol* 2005;25:2522–2527 doi: 10.1161/01.ATV.0000189298.62240.5d [PubMed: 16210570]
25. Yokoyama U, Minamisawa S, Quan H, Akaike T, Jin M, Otsu K, Ulucan C, Wang X, Baljinnam E, Takaoka M, et al. Epac1 is upregulated during neointima formation and promotes vascular smooth muscle cell migration. *Am J Physiol Heart Circ Physiol*. 2008;295:H1547–H1555. doi: 10.1152/ajpheart.01317.2007 [PubMed: 18689492]
26. Li Q, Teng Y, Wang J, Yu M, Li Y, Zheng H. Rap1 promotes proliferation and migration of vascular smooth muscle cell via the ERK pathway. *Pathol Res Pract*. 2018;214:1045–1050. doi: 10.1016/j.prp.2018.04.007 [PubMed: 29789158]
27. Wang Y, Su B, Xia Z. Brain-derived neurotrophic factor activates ERK5 in cortical neurons via a Rap1-MEKK2 signaling cascade. *J Biol Chem*. 2006;281:35965–35974. doi: 10.1074/jbc.M605503200 [PubMed: 17003042]
28. Wilhelmssen K, Mesa KR, Lucero J, Xu F, Hellman J. ERK5 protein promotes, whereas MEK1 protein differentially regulates, the Toll-like receptor 2 protein-dependent activation of human endothelial cells and monocytes. *J Biol Chem*. 2012;287:26478–26494. doi: 10.1074/jbc.M112.359489 [PubMed: 22707717]
29. Blanc A, Pandey NR, Srivastava AK. Synchronous activation of ERK 1/2, p38mapk and PKB/Akt signaling by H2O2 in vascular smooth muscle cells: potential involvement in vascular disease (review). *Int J Mol Med*. 2003;11:229–234. [PubMed: 12525883]
30. Priego N, Arechederra M, Sequera C, Bragado P, Vázquez-Carballo A, Gutiérrez-Uzquiza Á, Martín-Granado V, Ventura JJ, Kazanietz MG, Guerrero C, et al. C3G knock-down enhances migration and invasion by increasing Rap1-mediated p38α activation, while it impairs tumor growth through p38α-independent mechanisms. *Oncotarget*. 2016;7:45060–45078. doi: 10.18632/oncotarget.9911 [PubMed: 27286263]
31. Renna NF, de Las Heras N, Miatello RM. Pathophysiology of vascular remodeling in hypertension. *Int J Hypertens*. 2013;2013:808353. doi: 10.1155/2013/808353 [PubMed: 23970958]
32. Freitas Lima LC, Braga VA, do Socorro de França Silva M, Cruz JC, Sousa Santos SH, de Oliveira Monteiro MM, Balarini CM. Adipokines, diabetes and atherosclerosis: an inflammatory association. *Front Physiol*. 2015;6:304. doi: 10.3389/fphys.2015.00304 [PubMed: 26578976]
33. Amrani Y, Lazaar AL, Panettieri RA Jr. Up-regulation of ICAM-1 by cytokines in human tracheal smooth muscle cells involves an NF-kappa B-dependent signaling pathway that is only partially sensitive to dexamethasone. *J Immunol*. 1999;163:2128–2134. [PubMed: 10438953]
34. Song J, Duncan MJ, Li G, Chan C, Grady R, Stapleton A, Abraham SN. A novel TLR4-mediated signaling pathway leading to IL-6 responses in human bladder epithelial cells. *PLoS Pathog*. 2007;3:e60. doi: 10.1371/journal.ppat.0030060 [PubMed: 17465679]
35. Lee JH, Kim H, Woo JH, Joe EH, Jou I. 5, 8, 11, 14-eicosatetraenoic acid suppresses CCL2/MCP-1 expression in IFN-γ-stimulated astrocytes by increasing MAPK phosphatase-1 mRNA stability. *J Neuroinflammation*. 2012;9:34. doi: 10.1186/1742-2094-9-34 [PubMed: 22339770]
36. Gao L, Gülcüler GS, Golbach L, Block H, Zarbock A, Martin-Villalba A. Endothelial cell-derived CD95 ligand serves as a chemokine in induction of neutrophil slow rolling and adhesion. *Elife*. 2016;5:e18542. doi: 10.7554/eLife.18542 [PubMed: 27763263]
37. Sprynger M, Rigo F, Moonen M, Aboyans V, Edvardsen T, de Alcantara ML, Brodmann M, Naka KK, Kownator S, Simova I, et al.; EACVI Scientific Documents Committee. Focus on echovascular imaging assessment of arterial disease: complement to the ESC guidelines (PARTIM 1) in collaboration with the Working Group on Aorta and Peripheral Vascular Diseases. *Eur Heart J Cardiovasc Imaging*. 2018;19:1195–1221. doi: 10.1093/ehjci/jey103 [PubMed: 30239635]
38. Thomas KN, Lewis NC, Hill BG, Ainslie PN. Technical recommendations for the use of carotid duplex ultrasound for the assessment of extracranial blood flow. *Am J Physiol Regul Integr Comp Physiol*. 2015;309:R707–R720. doi: 10.1152/ajpregu.00211.2015 [PubMed: 26157060]

39. Acosta-Martin AE, Chwastyniak M, Beseme O, Drobecq H, Amouyel P, Pinet F. Impact of incomplete DNase I treatment on human macrophage proteome analysis. *Proteomics Clin Appl*. 2009;3:1236–1246. doi: 10.1002/prca.200900113 [PubMed: 21136947]
40. Shevchenko A, Jensen ON, Podtelejnikov AV, Sagliocco F, Wilm M, Vorm O, Mortensen P, Shevchenko A, Boucherie H, Mann M. Linking genome and proteome by mass spectrometry: large-scale identification of yeast proteins from two dimensional gels. *Proc Natl Acad Sci U S A*. 1996;93:14440–14445. doi: 10.1073/pnas.93.25.14440 [PubMed: 8962070]
41. Giannotta M, Benedetti S, Tedesco FS, Corada M, Trani M, D'Antuono R, Millet Q, Orsenigo F, Gálvez BG, Cossu G, et al. Targeting endothelial junctional adhesion molecule-A/ EPAC/ Rap-1 axis as a novel strategy to increase stem cell engraftment in dystrophic muscles. *EMBO Mol Med*. 2014;6:239–258. doi: 10.1002/emmm.201302520 [PubMed: 24378569]
42. Vergori L, Lauret E, Soleti R, Andriantsitohaina R, Carmen Martinez M. Microparticles carrying peroxisome proliferator-activated receptor alpha restore the reduced differentiation and functionality of bone marrow-derived cells induced by high-fat diet. *Stem Cells Transl Med*. 2018;7:135–145. doi: 10.1002/sctm.17-0098 [PubMed: 29080294]
43. Leroyer AS, Isobe H, Lesèche G, Castier Y, Wassef M, Mallat Z, Binder BR, Tedgui A, Boulanger CM. Cellular origins and thrombogenic activity of microparticles isolated from human atherosclerotic plaques. *J Am Coll Cardiol*. 2007;49:772–777. doi: 10.1016/j.jacc.2006.10.053 [PubMed: 17306706]

Novelty and Significance

What Is Known?

- Circulating levels of large extracellular vesicles (IEVs) are increased in metabolic syndrome (MetS) patients and participate in endothelial dysfunction.
- Proliferation, migration, and proinflammatory cytokine secretion from vascular smooth muscle cells play a crucial role in vascular remodeling, a key step in atherosclerosis progression.

What New Information Does This Article Contribute?

- IEVs from MetS patients carry the small GTPase Rap1, and levels of Rap1-IEVs correlate with cardiovascular risk, including stenosis.
- MetS-IEVs promote the migration and proliferation of human aortic smooth muscle cells and increase expression of proinflammatory cytokines via a Rap1-dependent mechanism.
- IEVs accumulate in plaque atherosclerotic lesions in both mice and humans.

Although it is known that extracellular vesicles participate in atherosclerosis by inducing endothelial dysfunction and proliferation of smooth muscle cells, less is known about IEVs from MetS patients. We performed a proteomic analysis of the content of these IEVs and identified increased levels of Rap1 in IEVs from MetS patients compared with controls. Notably, IEVs accumulate in atheroma plaque and Rap1-expressing IEVs exhibit proatherosclerotic functions, including enhancing migration, proliferation, and proinflammatory cytokine expression of vascular smooth muscle cells. These data define Rap1⁺-IEVs produced in excess as a potential therapeutic target to prevent or limit the progression of atherosclerosis in MetS subjects, as well as a potential biomarker to predict vascular consequences of MetS.

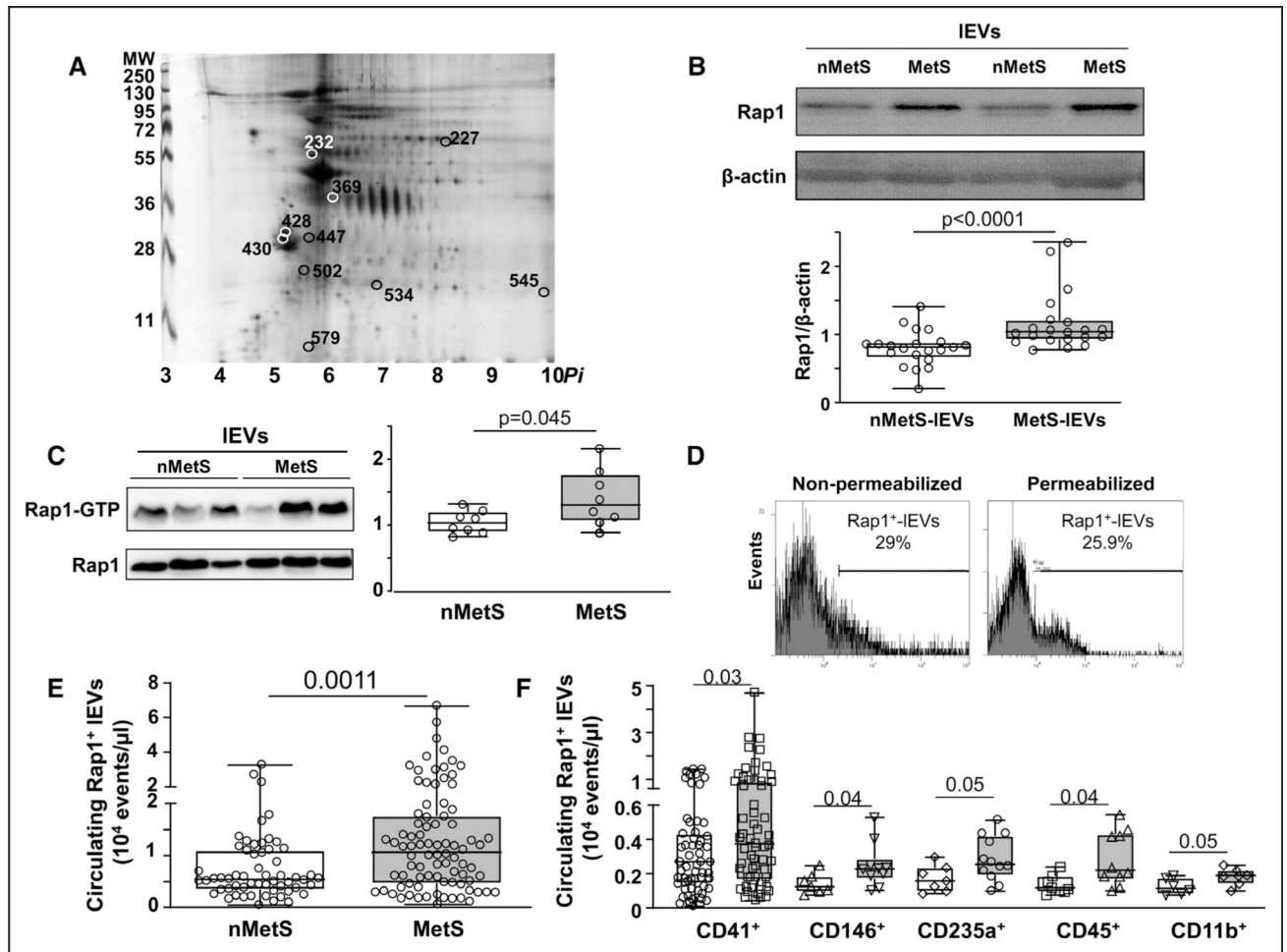


Figure 1. Characterization of large extracellular vesicles (IEVs) from non-metabolic subjects (nMetS) and metabolic syndrome (MetS) patients.

A, Representative 2D-DIGE (difference gel electrophoresis) gel and bioinformatic analysis of polypeptidic spots; circles are corresponding to those differentially abundant in IEVs from nMetS and MetS subjects. The positions of molecular weight (MW) pattern is indicated on the left and the isoelectric point (*Pi*) on the bottom of the gels ($n=5$). **B**, Representative Western blot of Rap1 protein expression in IEVs from nMetS and MetS subjects. Rap1 expression was significantly higher in MetS-IEVs ($n=21$) compared with nMetS-IEVs ($n=21$). **C**, Representative immunoblot of Rap1 pull-down experiments and quantification of Rap1-GTP ($n=8$). Rap1-GTP levels were significantly higher in MetS-IEVs. **D**, Differential Rap1 expression was analyzed on native and permeabilized MetS-IEVs by flow cytometry. Nonsignificant change was observed in Rap1 labeling after permeabilization ($n=8$). **E**, Circulating IEV levels expressing Rap1 in patients with MetS ($n=90$) compared with nMetS patients (nMetS $n=72$). **F**, Cellular origins of Rap1⁺-IEVs in nMetS (white) and MetS (gray) patients. CD41 ($n=55$ and $n=75$), CD146 ($n=7$ and $n=10$), CD235a ($n=7$ and $n=12$), CD45 ($n=7$ and $n=10$), and CD11b ($n=6$ and $n=7$) for nMetS and MetS, respectively. Data are shown as medians and interquartile ranges (IQRs) of numbers of IVs. *P* values in **B**, **C**, **E** were determined by the Mann-Whitney *U* test; **F**, Kruskal-Wallis test with Dunn test post

hoc between all conditions. *P* values were not indicated when nonsignificant Representative images were selected to represent the mean value of each condition.

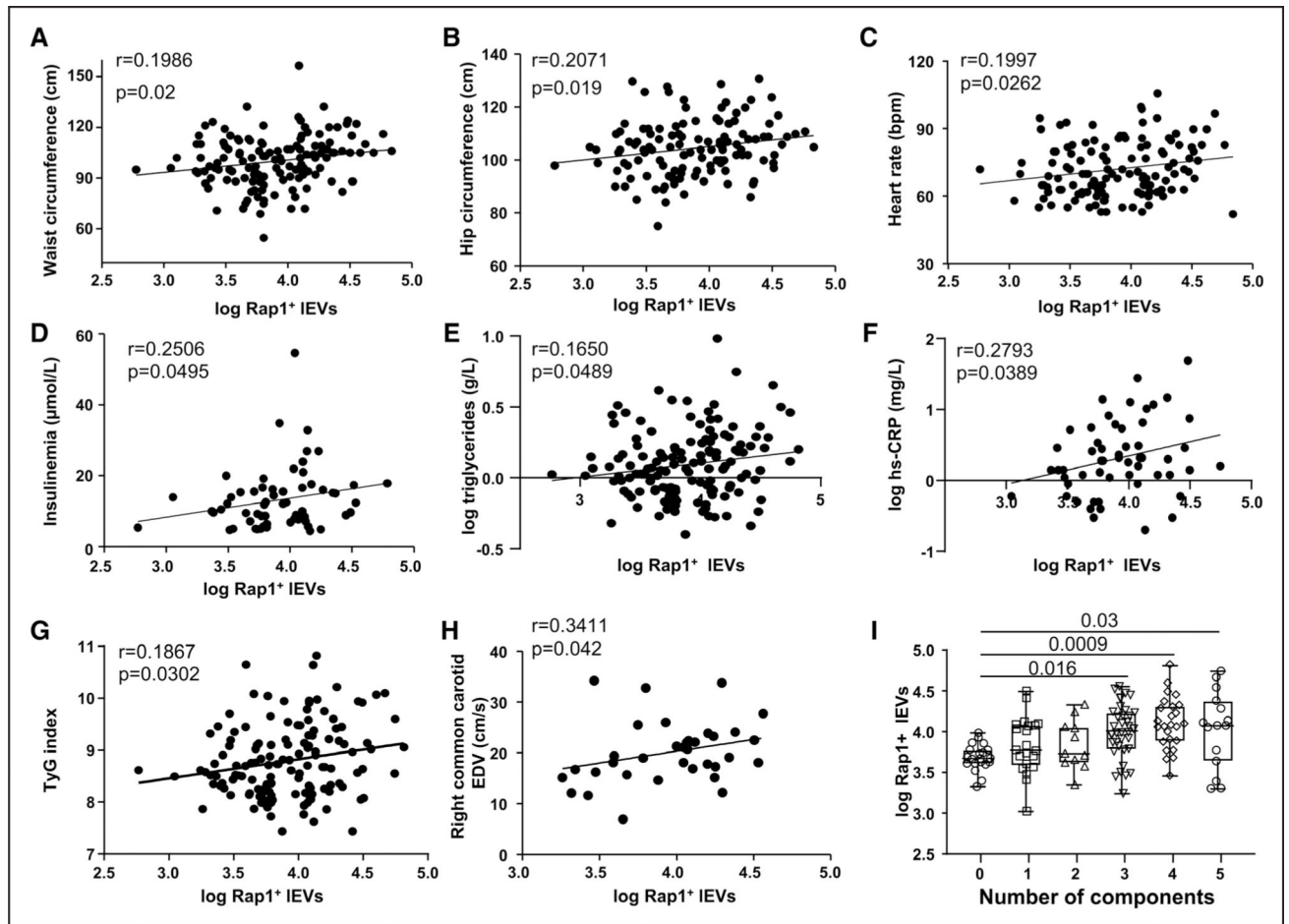


Figure 2. Correlation between circulating levels of Rap1-large extracellular vesicles (IEVs) and clinical findings observed in non-metabolic (nMetS) and metabolic syndrome (MetS) subjects. Correlations were performed between levels of Rap1 expression in IEVs and waist circumference (cm) (A), hip circumference (cm) (B), mean heart rate expressed in beats per minute (bpm) (C), insulinemia (μmol/L) (D), plasma triglycerides levels (g/L) (E), hs-CRP (high-sensitivity C-reactive protein) levels (mg/L) (F), TyG (triglyceride-glucose) index (G), right common carotid end-diastolic velocity (EDV, cm/s) (H), and number of components of MetS (I). Rap1 levels in circulating IEVs were detected by flow cytometry and expressed in log. Data are shown as medians and IQRs of numbers of IEVs. A-H, Correlations were performed by Spearman correlation test. For I, P values were determined by the Kruskal-Wallis test with Dunn test post hoc between all conditions. P values were not indicated when nonsignificant.

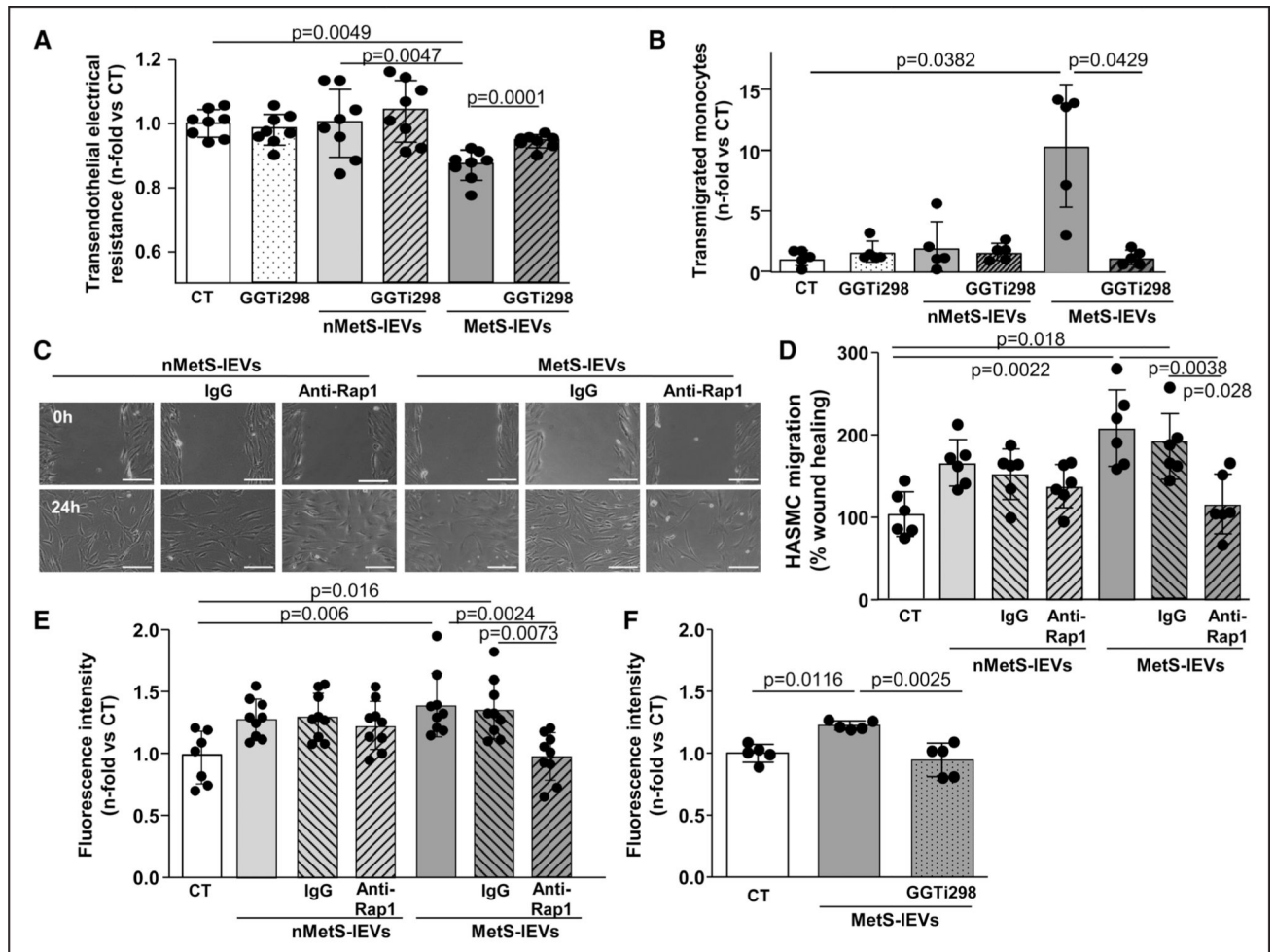


Figure 3. Circulating large extracellular vesicles (IEVs) increases endothelial permeability, migration, and proliferation of human aortic smooth muscle cells (HASMC).

A, Changes on endothelial permeability measured by transendothelial electrical resistance induced by IEVs from non-metabolic syndrome (nMetS) subjects or MetS patients preincubated or not with the Rap1 inhibitor GGTi-298 (60 $\mu\text{mol/L}$; n=8). **B**, Transmigration of THP-1 monocytes through an endothelial monolayer induced by IEVs from nMetS subjects or MetS patients preincubated or not with the Rap1 inhibitor GGTi-298 (n=5). **C**, Representative microscopy images and **(D)** quantification of HASMC migration were analyzed by wound healing assay at 0 h and after 24 h of treatment with nMetS-IEVs or MetS-IEVs preincubated or not either with anti-Rap1 antibody or its control IgG (n=6). Horizontal bar=200 μm . **E**, Effects of nMetS-IEVs and MetS-IEVs on number of HASMC measured by CyQuant Kit. Histograms show fluorescence intensity representing the changes on cell number induced by IEVs preincubated either with anti-Rap1 or its control IgG (n=9). **F**, Histograms show fluorescence intensity representing the changes on cell number induced by MetS-IEVs preincubated with the inhibitor of the Rap1 activity GGTi-298 and measured by CyQuant Kit (n=5). Data are shown as mean \pm SD. *P* values were determined by the Kruskal-Wallis test with Dunn test post hoc between all conditions for each panel. *P* values

were not indicated when nonsignificant. Representative images were selected to represent the mean value of each condition.

Author Manuscript

Author Manuscript

Author Manuscript

Author Manuscript

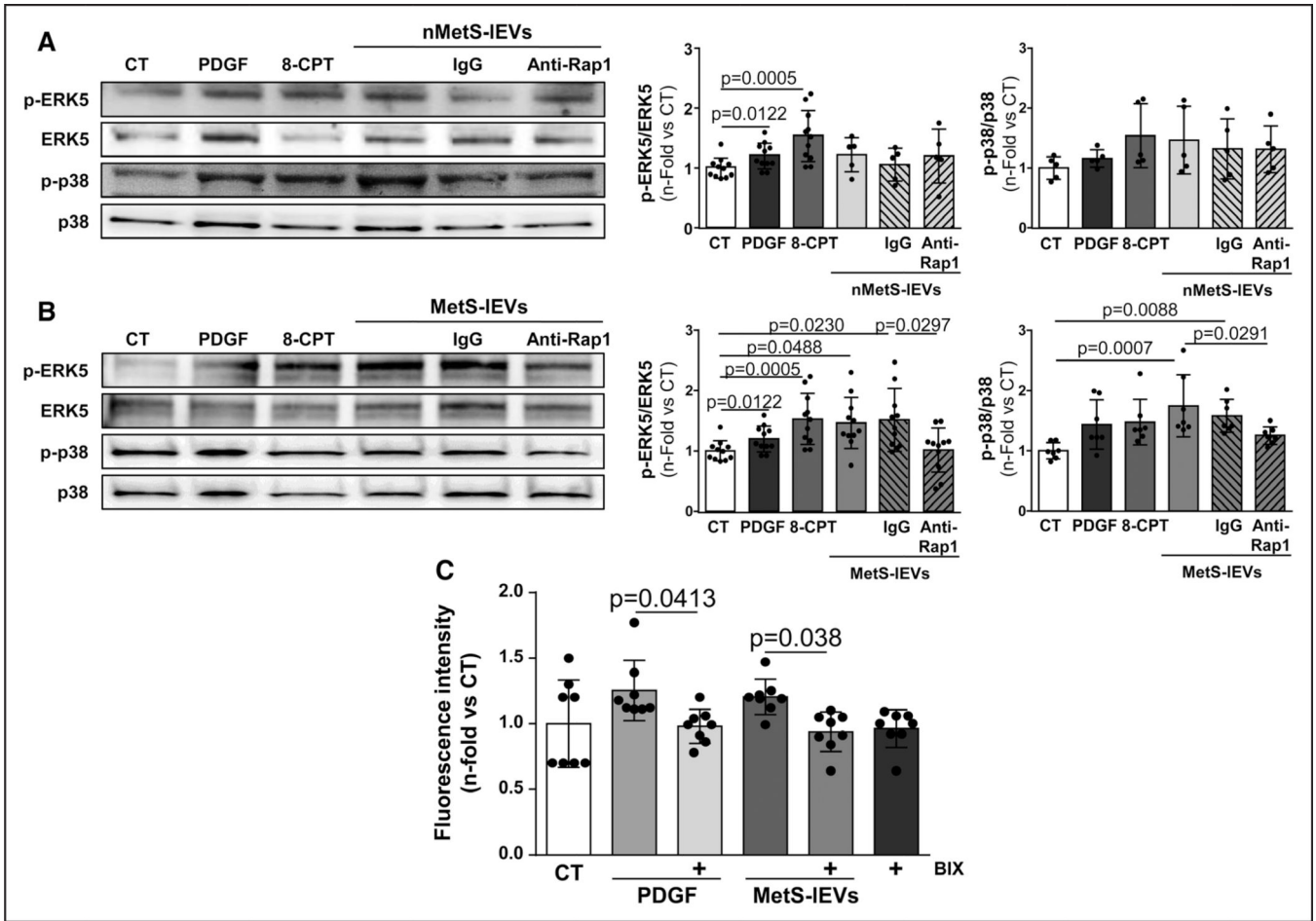


Figure 4. Rap1 carried by large extracellular vesicles (IEVs) regulates activation of MEK5-ERK5 and p38 pathways to induce proliferation of human aortic smooth muscle cells (HASMC).

A and B, Representative immunoblot and quantification of ERK (extracellular signal-regulated kinase) 5 and p38 activation induced by PDGF (platelet-derived growth factor), 8-(4-Chlorophenylthio) adenosine 3',5'-cyclic monophosphate sodium salt (8-CPT), non-metabolic syndrome (nMetS)-IEVs (n=5) or MetS-IEVs (n=11). IEVs were preincubated with anti-Rap1 antibody or its control IgG. **C,** Histograms showing fluorescence intensity representing the cell number of HASMC induced by either PDGF or MetS-IEVs in the absence or presence of BIX, a MEK5-ERK5 inhibitor (n=8). Data are shown as mean±SD. *P* values were determined by the Kruskal-Wallis test with Dunn test post hoc between all conditions for each panel. *P* values were not indicated when nonsignificant. Representative immunoblots were selected to represent the mean value of each condition.

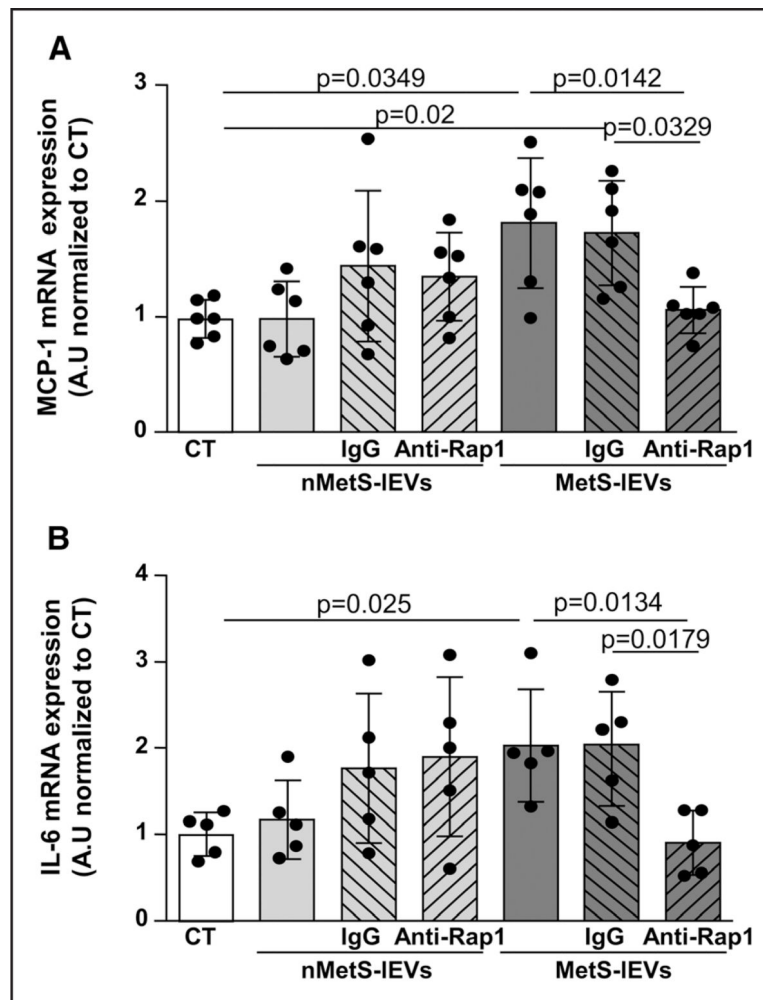


Figure 5. Metabolic syndrome large extracellular vesicles (MetS-IEVs) increase MCP (monocyte chemoattractant protein)-1 and IL (interleukin)-6 expression in a Rap1-dependent manner. Relative transcript expression of the inflammatory cytokines MCP-1 (**A**) (n=6) and IL-6 (**B**) (n=5) in human aortic smooth muscle cells (HASMC) after 14 h induction by non-MetS (nMetS)-IEVs or MetS-IEVs preincubated either with anti-Rap1 or its control IgG. Data are shown as mean±SD. *P* values were determined by the Kruskal-Wallis test with Dunn test post hoc between all conditions for each panel. *P* values were not indicated when nonsignificant.

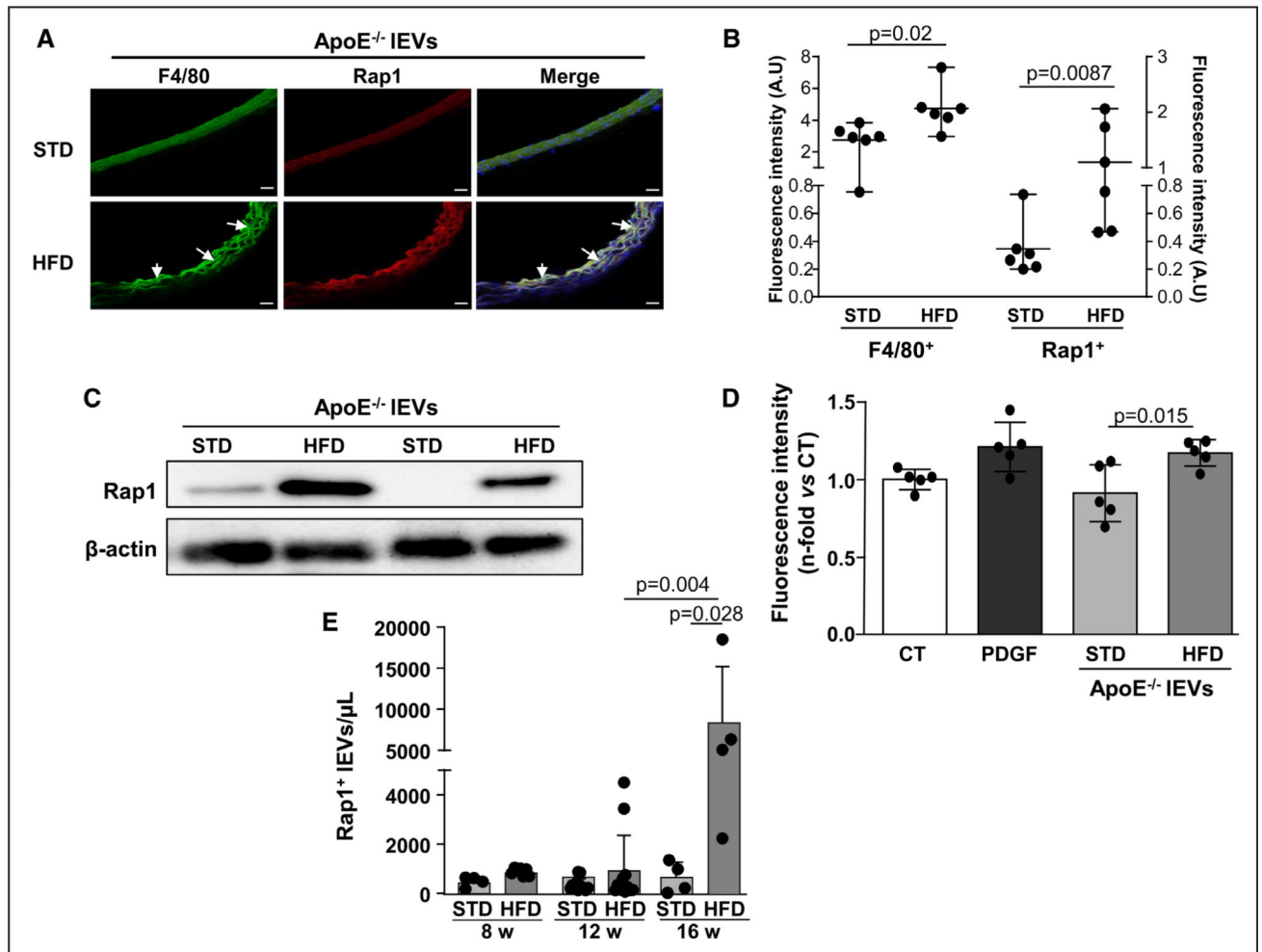


Figure 6. Rap1 expression in circulating large extracellular vesicles (IEVs) and in atheroma IEVs from high-fat diet (HFD)-fed ApoE^{-/-} mice.

A, Representative confocal immunofluorescence images of aortic roots from standard diet (STD)- or HFD-fed ApoE^{-/-} mice stained with the macrophage marker F4/80 (green staining) and Rap1 (red staining). DAPI staining localized nuclei of cells in aortic roots (blue staining). Horizontal bar=20 μ m. White arrows show macrophages in the intima plaque from HFD ApoE^{-/-} mice. **B**, Quantification of F4/80 staining and Rap1 immunofluorescence of aortic roots from STD- or HFD-fed ApoE^{-/-} mice. Fluorescence intensity was expressed in arbitrary units (n=6). **C**, Protein expression of Rap1 in IEVs from STD- or HFD-fed ApoE^{-/-} mice (n=2). **D**, Histograms show rates of mouse aortic smooth muscle cells (SMC) number induced by IEVs from HFD-fed ApoE^{-/-} mice (n=5). **E**, Quantification of Rap1⁺-IEVs isolated from aortic wall from STD-fed ApoE^{-/-} mice and from atherosclerotic aortic lesions from ApoE^{-/-} mice fed with HFD for 8 (n=4 for STD and n=7 for HFD), 12 (n=12) or 16 wk (n=4). Data are shown as mean \pm SD. *P* values in **B**, **D** were determined by the Mann-Whitney *U* test; **E**, Kruskal-Wallis test with Dunn test post hoc between all conditions. *P* values were not indicated when nonsignificant. Representative images were selected to represent the mean value of each condition.

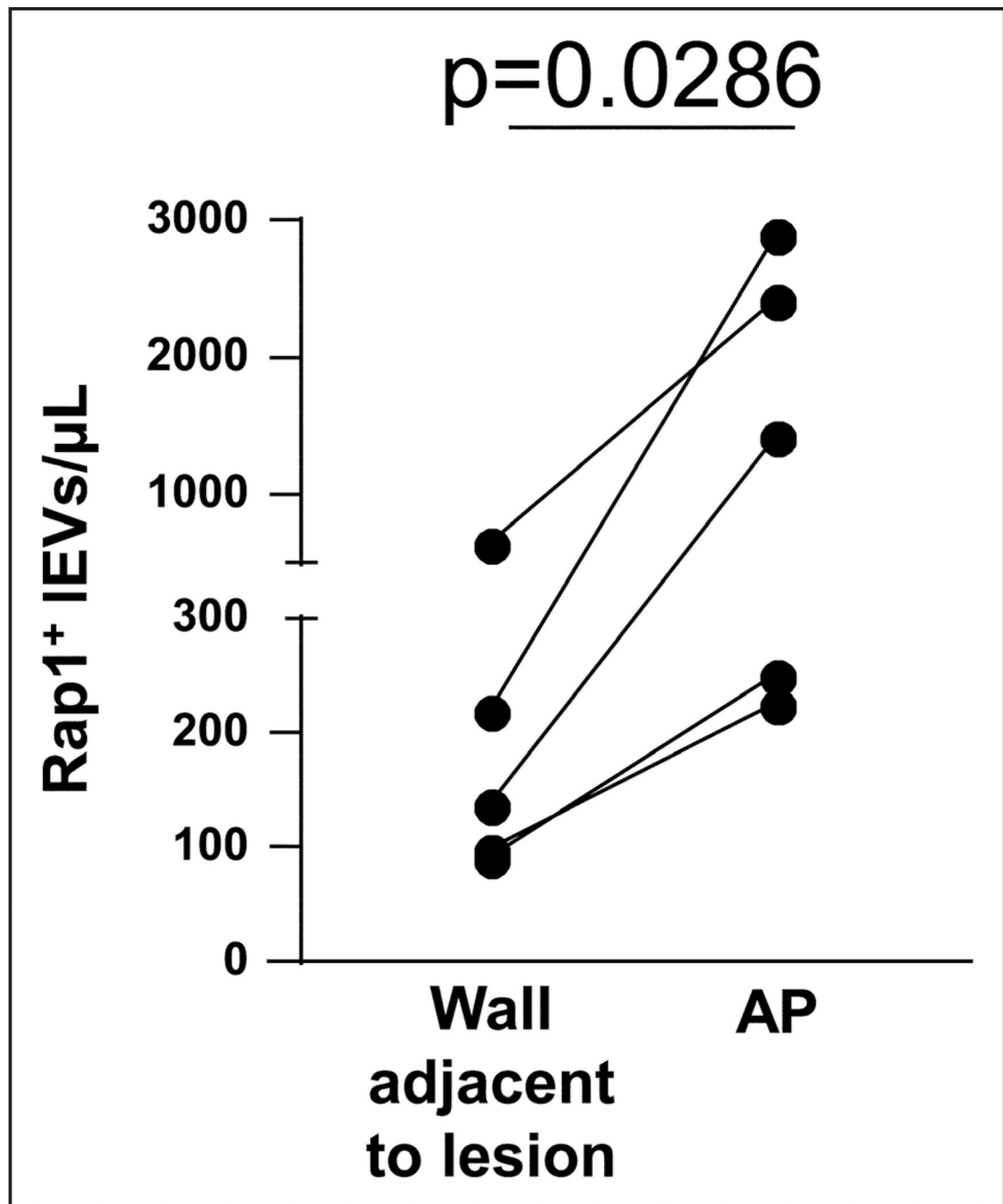


Figure 7. Rap1 expression in large extracellular vesicles (IEVs) isolated from human atherosclerotic plaques.

Quantification of Rap1⁺-IEVs isolated from atherosclerotic plaques (AP) and from the arterial wall adjacent to the lesion from patients undergoing carotid endarterectomy (n=5). Data are shown as interconnected dots between conditions for each related sample. *P* value was determined by the Mann-Whitney *U* test.